A Method of Second-order Propagation Delay Correction in Real-time Precise Positioning

M. Mainul Hoque[1], **N. Jakowski**[2]
German Aerospace Center (DLR)
Institute of Communications and Navigation
D-17235 Neustrelitz, Germany
Fax: ++49 3981480123
[1]Email: Mainul.Hoque@dlr.de
[2]Email: Norbert.Jakowski@dlr.de

Abstract. Dual frequency GPS measurements cannot fully compensate higher order ionospheric refraction effects and lead to a residual error in the so-called "ionosphere free" L_3 linear phase combination. Due to the dependency on the geomagnetic field, the second-order residual error is highly variable with elevation and azimuth angles and difficult to model. However, based on ionospheric simulations using the Chapman function and a superposed exponential decay for describing the vertical electron density distribution, we developed a correction formula for the second-order residual phase error. Analysis shows that our proposed correction formula limits the second-order propagation effect less than 2 mm residual range error for GNSS users in Germany.

1. Introduction

Due to the dispersive nature of the ionosphere, the first-order propagation error may fully be corrected by differencing the signal at two spaced frequencies. But whereas the first order effect may be completely removed, the higher order effects are not fully compensated by the difference method. The second-order residual error can vary from a few millimeters to several centimeters depending on the elevation angle, the geographic location and solar-terrestrial relationships.

Brunner and Gu (1991) propose a formula of dual frequency ionospheric correction which limits the ionospheric higher order effects less than 1 mm residual range error. However, it requires the knowledge of the actual maximum electron density, N_m an ionospheric electron density profile shape factor, η and the average value of the longitudinal component of the earth's magnetic field along the ray path, $\overline{B\cos\Theta}$. In practical cases these parameters are not easy to estimate. Bassiri and Hajj (1993) propose an approximation to correct the second-order effect which has an average error of 0.11 cm and a variance of 0.25 cm in group delay measurements. However, they assume an earth-centered tilted dipole approximation for the geomagnetic field which is in general only accurate to about 75%. As already demonstrated for VLBI (Hawarey et al. 2005) further improvements for the 2nd–order ionospheric term can be achieved using more realistic magnetic field model such as the International Geomagnetic Reference Field (IGRF) instead of a dipole model.

This paper investigates the effects of the magneto-ionic interaction, but still neglects the differential bending of the signals which exceeds the magneto-ionic errors at very low elevation angles (Jakowski et al. 1994).

2. Radio Wave Propagation in the Ionosphere

The high frequency (HF) radio signal transmitted by the satellite passes through plasmasphere/ionosphere and is subjected to the ionospheric refraction (see Figure 1). The geometric path length or true range ρ between the transmitting satellite and the receiver is-

$$\rho = \quad L \quad + \int_S^R (1-n)ds \quad - \Delta s_B \qquad (1)$$

optical distance | phase delay error | ray path bending error

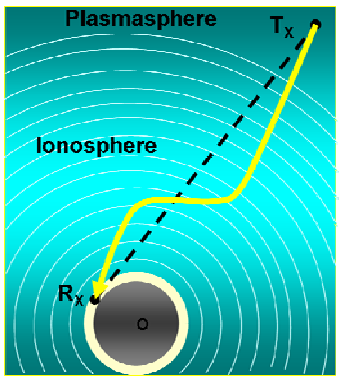

Figure 1: The radio wave propagation through ionosphere.

where n is the ionosphere phase refractive index and ds is the ray path element. The phase delay error is much more significant over the ray path bending error Δs_B; but the latter may play a certain role in high precision positioning especially at low elevation angles. For reasons of simplicity, the ray path bending effect is ignored in the following computation of the second-order ionospheric refraction effects i.e. the effects are computed along the line of sight propagation (LOS). This procedure is justified because the second-order effect of a second-order effect will be less than the computational accuracy of the ray-tracing technique and can be neglected.

2.1 Refractive Index and Higher-Order Effects

The radio wave propagation through the ionosphere is well described in the fundamental literature (e.g. Budden 1985, Davies 1990). The refractive index of the ionosphere at GPS frequencies, as given by Brunner and Gu (1991), neglecting those terms whose magnitude is less than 10^{-9}, can be expressed as:

$$n = 1 - \frac{{f_p}^2}{2f^2} \pm \frac{f_p^2 f_g \cos\Theta}{2f^3} - \frac{f_p^4}{8f^4} \qquad (2)$$

Where Θ is the angle between the wave propagation direction and the geomagnetic field vector, f is the signal frequency, $f_p = \sqrt{e^2 n_e / (4\pi^2 m_e \varepsilon_0)}$ is the plasma frequency, $f_g = eB/(2\pi m_e)$ is the electron gyro frequency, ε_0 is the free space permittivity, B is the geomagnetic induction and e, n_e and m_e are electron charge, density and mass, respectively. The wave with the upper (+) sign in (2) is usually called the 'ordinary' wave whereas the lower (-) sign is related to the 'extraordinary' wave. The ordinary mode is left-hand circularly polarized while the extra-ordinary mode is right-hand circularly polarized (Hartmann and Leitinger 1984). Since GPS signals are generally transmitted at right-hand polarization (Parkinson and Gilbert 1983) only the results of extra-ordinary mode are given in this paper.

Combining the ionospheric phase delay expression (2nd term of right side of (1)) with the refractive index formula (2), the second order phase delay term can be separated as-

$$d_I^{(2)} = \frac{K_B}{f^3} \int_S^R B\cos\Theta \cdot n_e ds \qquad (3)$$

where, $K_B = 1.1281 \times 10^{12}$ $m^3 s^{-1} A kg^{-1}$.

The GNSS carrier phase Φ at a selected frequency can be described by the observation equation (in units of length):

$$\Phi = \rho + c(dt - dT) - d_I + d_A + d_{MP} + dq + dQ + N\lambda + \varepsilon_\Phi \tag{4}$$

where c is the velocity of light, dt and dT are satellite and receiver clock errors, respectively, d_A is the atmospheric (tropospheric) delay, d_{MP} is the error due to multipath, dq and dQ are instrumental biases of the satellite and receivers, respectively, λ is the carrier wave length, N is the phase ambiguity number (integer) and ε_Φ is the rest error.

As we confine our interest only on higher order effects the observation equation is simplified accordingly in the following "ionosphere free" L_3 linear phase combination.

$$\Phi_3 = (1 + \beta_3)\Phi_1 - \beta_3 \Phi_2 = \rho + \Delta s_2 \tag{5}$$

In which,

$$\Delta s_2 = \frac{K_B}{f_1 f_2 (f_1 + f_2)} \int_S^R B \cos\Theta \cdot n_e ds \tag{6}$$

where, Φ_1 and Φ_2 are phase observables at GPS f_1 (1575 MHz) and f_2 (1228 MHz) frequencies, respectively, $\beta_3 = f_2^2 / (f_1^2 - f_2^2)$ is called the ionospheric scaling factor and Δs_2 is the second-order residual phase error. For the GPS pair of frequencies, β_3 is 1.546. To estimate Δs_2 we have applied numerical tracing to numerous magneto-ionic conditions having different azimuth and elevation angles of the radio link.

2.2 Ionospheric Layers and Geomagnetic Field Model

To compute the higher-order delays, we have to assume models for the electron density n_e and the earth's magnetic field B. The electron density profiles of the ionosphere/plasmasphere are generated by the generalized Chapman profile formula (Jakowski et al. 1994) with a superimposed simple exponential decay function from an altitude (~ 1000 km) well above the F2-layer height *hmF2*.

$$n_e(h) = NmF2 \exp\left(\frac{1}{2}(1 - z - \exp(-z))\right) + n_p \exp\left(-\frac{h}{H_s^P}\right) \tag{7}$$

In which $z = (h - hmF2) / H_s^I$ and $NmF2 = 1.24 \times 10^{-2} (foF2)^2$ where H_s^I (~60-80 km) and H_s^P (~10000 km) are ionosphere and plasmasphere mean scale heights, respectively, *NmF2* is the peak electron density at the F2-layer height $hmF2$ (~250-450 km) and $foF2$ is the critical ionosonde frequency.

For simplicity, we still ignore the ray path bending effect, so that the direction of the signal propagation path can be assumed to be constant along its entire path, which is from the satellite to the receiver in the 3D space (see Figure 2).

The International Geomagnetic Reference Field (IGRF) model (Mandea and Macmillan 2000) is used to compute the magnetic induction B along the ray path. The IGRF model provides geomagnetic field components in northward, eastward and vertically-downward directions which are translated into the generalized geocentric XYZ coordinate system to compute Θ, the angle between the wave propagation direction and the geomagnetic field vector.

The second-order residual error, Δs_2 can be either positive or negative as Θ varies in the range of 0-180° (see Figure 2) depending on the satellite-to-receiver link.

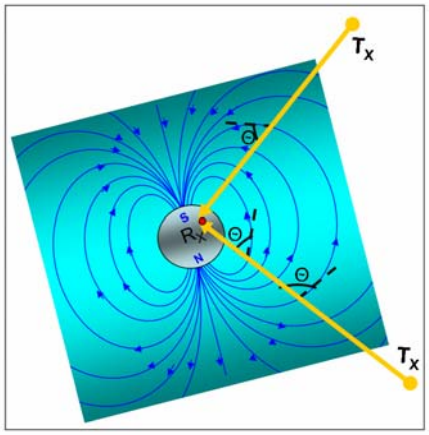

Figure 2: Magneto-ionic intersection.

3. Results Analysis

In this study we confine our interest on GNSS users in Germany. To get one proxy solution for German GNSS users, we take a reference user position, approximately in mid Germany, having the latitude ϕ_{Rx} = 51° N and the longitude λ_{Rx} = 10° E and the satellite orbit height h_{Tx} is considered as 20200 km (GPS, GLONASS).

In Figure 3 and Figure 4 (left plot) user-to-satellite azimuth angle is varied around a circle from 0-360° and elevation angle is varied from 0-90° whereas plots for elevation angles ε = 10°, 30° and 60° are separately marked. In Figure 3 the second-order phase errors at GPS L1 and L2 frequencies are represented by the radial distance from the center of the azimuth circle. The errors are found minimum in the northward direction (azimuth, α = 0) whereas the maximum values are observed in the southward direction (α =180°).

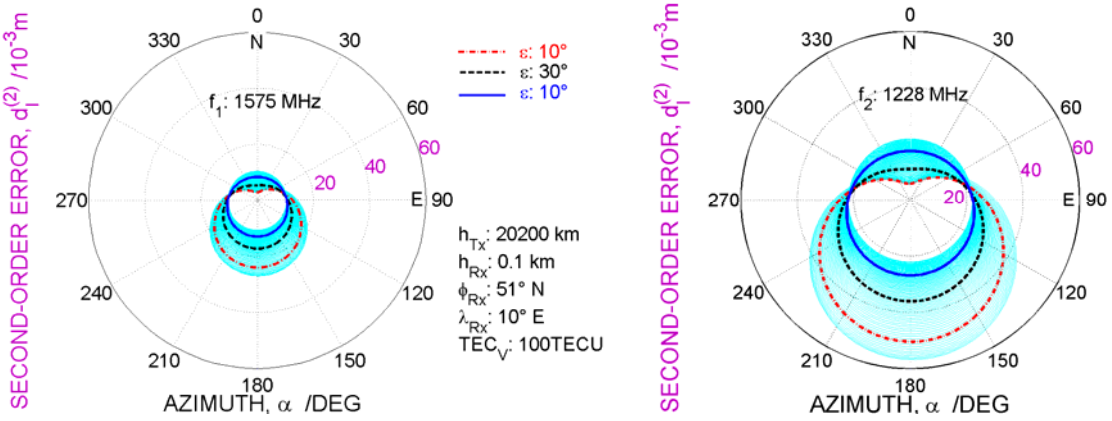

Figure 3: Variations of the second-order phase error with azimuth and elevation angles at GPS L1 and L2 frequencies.

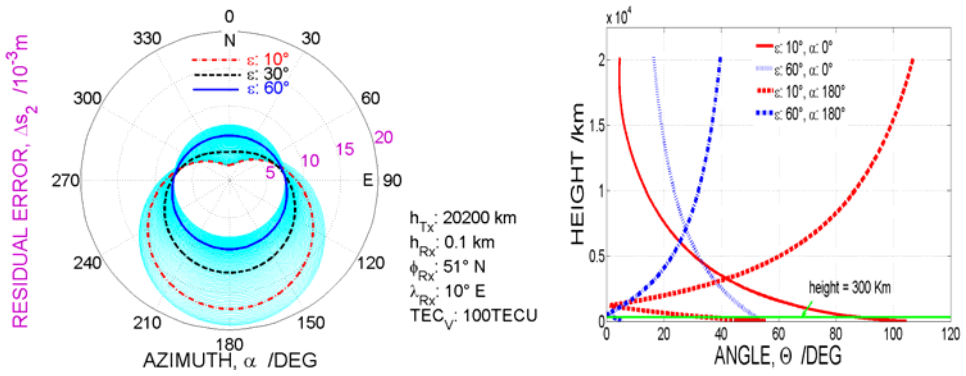

Figure 4: Variations of the second-order residual phase error with azimuth and elevation angles are shown in the left plot. The right plot shows the variation of Θ with height along line of sight propagation.

At a certain elevation angle, the difference in residual phase errors for different azimuth angles (see left plot of Figure 4) comes from the term $n_e B\cos\Theta$ of (6). It is known that the magnetic induction is inversely proportional to the cube of the distance from the earth's center. Moreover, the ionosphere electron density reaches its peak value at *hmF2* height and decreases exponentially with the increase of altitude. Thus, the product $n_e B\cos\Theta$ at the lower height (near *hmF2*) dominates the outcome of (6). For azimuth, $\alpha = 180°$ the contribution of these products is higher than for $\alpha = 0°$ due to the smaller value of Θ at ionospheric altitudes less than 1000 km (see right plot of Figure 4).

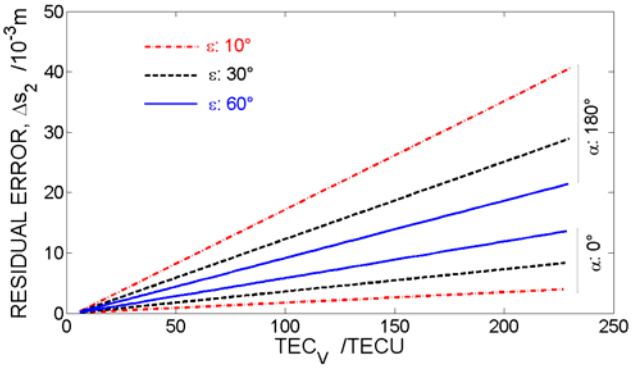

Figure 5: Dependency of the second-order residual error on the vertical total electron content, TEC_V.

The second-order residual phase error has a linear dependency on the vertical total electron content, TEC_V (see Figure 5). At azimuth $\alpha = 180°$ the plots are steeper at lower elevations i.e. Δs_2 increases at a higher rate with TEC_V at lower elevation angle. The scenario is reversed at $\alpha = 0°$ i.e. Δs_2 increases at a higher rate with TEC_V at higher elevation angle.

4. Correction Formula

For a certain elevation angle (e.g. $\varepsilon = 10°$), the second-order residual phase error varies with azimuth angles in the form of a regularly shaped closed curve. Similar curves are obtained for the full elevation angle range 0-90°. Studies reveal that such a curve can be expressed by the linear difference of two circles whose centers lie on the vertical axis (0-180° azimuth axis, see Figure 6). Let the horizontal axis (90°-270° azimuth axis) is X and the vertical axis is Y. knowing the

radius and centers of both circles each closed curve can be retrieved by the triangular geometry as follows-

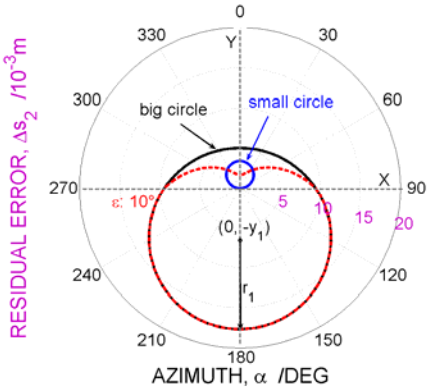

Figure 6: Two-circle-approximation.

$$\Delta s_2(\varepsilon,\alpha,TEC)=\left(-y_1\cos\alpha+\left|\sqrt{r_1^2-y_1^2\sin^2\alpha}\right|-2r_2\cos\alpha'\right)\cdot TEC \quad \text{[mm]} \qquad (8)$$

in which,

$$\begin{cases}\alpha'=\pi/2 & if \quad \pi/2<\alpha>3\pi/2\\ \alpha'=\alpha & otherwise\end{cases}$$

ε	elevation angle in degree
α	azimuth angle in radian
TEC	total electron content in TECU (1 TECU = 10^{16} electrons/m^2)

Where r_1 and r_2 are radius of the big and the small circles (see Figure 6), respectively, whose center coordinates lie at (0,-y_1) and (0,r_2). For the elevation range 0-90°; r_1, r_2 and y_1 values can be best fitted by three 4th order polynomials of elevation ε in a least square sense whose coefficients are written in Table 1.

$$\begin{aligned} r_1 &= \sum_{i=0}^{4} a_i.(\varepsilon)^i \\ r_2 &= \sum_{i=0}^{4} b_i.(\varepsilon)^i \\ y_1 &= \sum_{i=0}^{4} c_i.(\varepsilon)^i \end{aligned} \qquad (9)$$

i	***0***	***1***	***2***	***3***	***4***
a_i	4.1514305e-02	-1.9020325e-04	2.8470433e-05	-3.6603744e-07	1.3882738e-09
b_i	5.2909515e-03	1.0645432e-04	-7.5678609e-06	1.0305995e-07	-4.3889548e-10
c_i	2.3026249e-02	-1.7983094e-05	-3.0371937e-07	-5.1268669e-08	2.8083198e-10

Table 1: Higher order polynomial coefficients.

Thus, the second-order residual error can be directly derived by the proposed correction formula (8) knowing *TEC*, elevation, azimuth angles and as well as polynomial coefficients. This is the proposed second-order residual error correction formula which is truly valid for a GNSS user in mid Germany (latitude 51° N and longitude 10° E). Now the validation of this formula will be checked for whole Germany.

Validation of Correction Formula

Simulations are done at different geographic points over Germany to satisfy 1x1 latitude and longitude resolution (see Figure 7). The remaining errors (Δs_2 by LOS integration (6) – Δs_2 by correction formula (8)) are estimated at each point for elevation range 0-90° and azimuth range 0-360°.

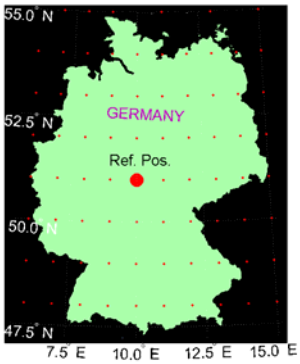

Figure 7: Reference position and simulation points (small dots) having 1x1 latitude and longitude resolution over Germany.

As already mentioned in section 2.2, the Chapman formula is used to compute the electron density along the signal path. In the following statistical analysis the ionospheric scale height *Hp* is randomly varied from 60-80 km and peak F2-layer height *hmF2* is varied from 250-350 km whereas the total electron content (TEC) is kept constant at 100 and 200 TECU (see Figure 8). This *hmF2* range is justified as we know the *hmF2* height rarely exceeds 350 km at mid latitude.

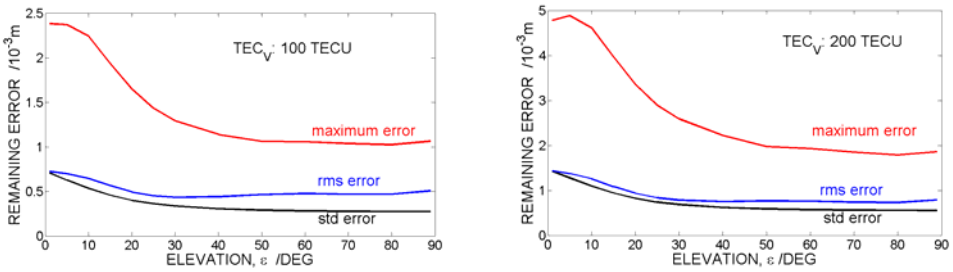

Figure 8: Statistical analysis of the remaining errors.

The root mean square (rms), the standard deviation (std) and the maximum value of remaining errors are estimated with respect to the elevation angle and independent of the azimuth angle (see Figure 8). The root mean square and the standard deviation of errors are well below 1 mm level whereas the maximum error exceeds 2 mm level at low elevation angles for a high vertical TEC of 100 TECU. Comparing the left and the right plot of Figure 8 it is found that the remaining error is directly proportional to the total electron content whatever the values of ionosphere scale height, H_p and peak F2-layer height *hmF2*.

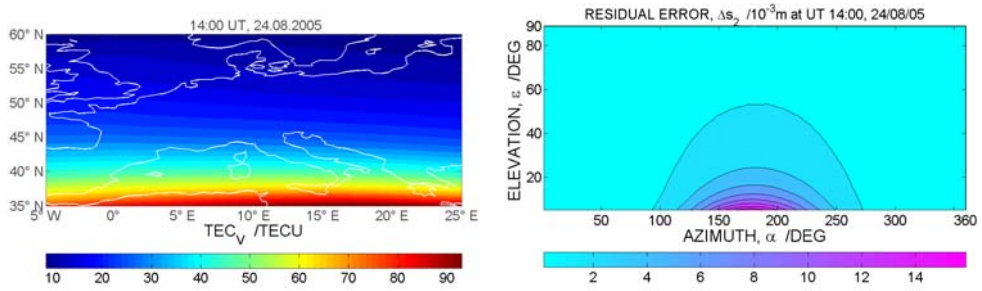

Figure 9: TEC map over Europe (left plot) and the second-order residual error map over Germany at UT 14:00 hour on 24th August 2005.

Figure 9 shows Δs_2 estimated by the correction formula over Germany when a high vertical TEC is observed over Europe (see left plot of Figure 9) at UT 14:00 hour on 24th August 2005.

5. Conclusion

Since the second and higher order errors are well below the meter level, they are commonly not considered in GPS positioning. However, if millimeter level accuracy is needed in precise navigation and positioning applications, the higher order effects cannot be ignored any more. Furthermore, satellite positions are affected at the centimeter level when applying the higher-order corrections (Fritsche et al. 2005). The proposed correction formula can be implemented in real-time applications as it does not require the knowledge of the geomagnetic field or the electron density distribution in the ionosphere along the signal path; only the total electron content (TEC) and geometrical parameters defining the ray path such as azimuth and elevation angles are required. It is expected that the correction will enable a more accurate positioning by using carrier phase measurements.

Acknowledgements. This work has been financially supported by the German State Government of Mecklenburg-Vorpommern under Grant V230-630-08-TIFA-334.

References

Bassiri S, Hajj G A. (1993) Higher-order Ionospheric Effects on the Global Positioning System Observables and Means of Modeling Them. Manuscripta Geodaetica 18: 280-289

Brunner F K, Gu M (1991) An Improved Model for the Dual Frequency Ionospheric Correction of GPS Observations. Manuscripta Geodaetica 16: 205-214

Budden KG (1985) The Propagation of Radio Waves: the theory of radio waves of low power in the ionosphere and magnetosphere. Cambridge University Press, Cambridge, ISBN 0 521 25461 2

Davies K (1990) Ionospheric Radio. Peter Peregrinus Ltd., London, UK, ISBN 0 86341 186 X

Fritsche M, Dietrich R, Knöfel C, Rülke A, Vey S, Rothacher M, Steigenberger P (2005) Impact of higher-order ionospheric terms on GPS estimates. Geophys Res Lett 32 doi: 10.1029/2005GL024342

Hartmann G K, Leitinger R (1984) Range errors due to ionospheric and tropospheric effects for signal frequencies above 100 MHz. B Geod 58: 109-136

Hawarey M, Hobiger T, Schuh H (2005) Effects of the 2nd order ionospheric terms on VLBI measurements, Geophys. Res. Lett., 32, L11304, doi: 10.1029/2005GL022729

Jakowski N, Porsch F, Mayer G (1994) Ionosphere-Induced-Ray-Path Bending Effects in Precise Satellite Positioning Systems. Zeitschrift für Satellitengestützte Positionierung, Navigation und Kommunikation, März 1994, pp. 6-13

Mandea M, Macmillan S (2000) International Geomagnetic Reference Field—the eighth generation, *Earth Planets Space*, Vol. 52, pp. 1119–1124, 2000

Parkinson B W, Gilbert S W (1983) NAVSTAR: Global Positioning System - Ten Years Later. Proc IEEE 71, pp 1177-1186